

# Cosmological inference from within the peculiar local universe

Roya Mohayaee<sup>1</sup> , Mohamed Rameez<sup>2</sup>  and Subir Sarkar<sup>3</sup> 

<sup>1</sup> CNRS, UPMC, Institut d'Astrophysique de Paris, 98 bis Bld Arago, Paris, France

<sup>2</sup> Tata Institute of Fundamental Research, Homi Bhabha Road, Mumbai 400005, India

<sup>3</sup> Rudolf Peierls Centre for Theoretical Physics, University of Oxford, Parks Road, Oxford OX1 3PU, UK

\* Correspondence: mohayaee@iap.fr

**Abstract:** The existence of ‘peculiar’ velocities due to the formation of cosmic structure marks a point of discord between the real Universe and the usually assumed Friedmann-Lemaître-Robertson-Walker metric which accommodates only the smooth Hubble expansion on large scales. In the standard  $\Lambda$ CDM model framework, Type Ia supernovae data are routinely “corrected” for the peculiar velocities of both the observer and the supernova host galaxies relative to the cosmic rest frame, in order to infer evidence for acceleration of the expansion rate from their Hubble diagram. However observations indicate a strong, coherent local bulk flow that continues outward without decaying out to a redshift  $z \gtrsim 0.1$ , contrary to the  $\Lambda$ CDM expectation. By querying the halo catalogue of the Dark Sky Hubble-volume N-body simulation, we find that an observer placed in an unusual environment like our local Universe should see correlations between supernovae in the JLA catalogue that are 2–8 times stronger than seen by a typical or Copernican observer. This accounts for our finding that peculiar velocity corrections have a large impact on the value of the Cosmological Constant inferred from supernova data. We also demonstrate that local Universe-like observers will infer a downward biased value of the clustering parameter  $S_8$  from comparing the density and velocity fields. More realistic modelling of the peculiar local Universe is thus essential for correctly interpreting cosmological data.

**Keywords:** cosmology:observations – cosmological parameters – cosmology:theory

## 1. Introduction

The flat  $\Lambda$ CDM ‘standard model’ of cosmology, which has a dominant fraction of its energy density  $\Omega_\Lambda \sim 0.7$  in the form of a Cosmological Constant and a fraction  $\Omega_m \sim 0.3$  in matter (of which  $\sim 85\%$  is cold dark matter and  $\sim 15\%$  baryons), is said to be a “good approximation to reality” [45]. It is nevertheless experiencing a crisis due to a significant tension between the value of the present expansion rate  $H_0$  ( $\equiv 100h \text{ km s}^{-1} \text{ Mpc}$ ,  $h \simeq 0.7$ ) determined using the ‘cosmic distance ladder’ anchored in the local universe, and the value inferred from the Cosmic Microwave Background (CMB) in the  $\Lambda$ CDM model framework [21]. Another tension is between the growth parameter  $S_8 = \sigma_8(\Omega_m/0.3)^{0.5}$  determined from observations of weak gravitational lensing, and from CMB data, where  $\sigma_8$  is the variance of mass fluctuations in a top-hat sphere of radius  $8h^{-1} \text{ Mpc}$  [1].

In the  $\Lambda$ CDM model data is interpreted using the Friedmann-Lemaître equations, obtained from General Relativity assuming the Cosmological Principle. In its modern form this assumes statistical isotropy and homogeneity in the distribution of matter and radiation in the ‘cosmic rest frame’ (CRF) in which the CMB dipole, assumed to be of kinematical origin, is presumed to vanish. We have recently shown however that the distribution of distant matter as traced by quasars and radio galaxies is *not* isotropic in the CRF [54,55], thus challenging this foundational assumption of the Friedmann-Lemaître-Robertson-Walker metric. We have also shown that the acceleration of the Hubble expansion rate inferred from Type Ia supernovae (SNe Ia) is *anisotropic* in the heliocentric frame so cannot be interpreted as due to  $\Lambda$  [12]. It is likely an artefact [58] because of our being ‘tilted’ observers embedded in a coherent bulk flow which gives rise to the prominent dipole anisotropy in the CMB. Moreover the local bulk flow extends out significantly further than is expected in the standard  $\Lambda$ CDM model, and no convergence is seen to the CRF out as



**Citation:** Mohayaee, R.; Rameez, M.; Sarkar, S. Peculiar local Universe. *Preprints* 2023, 1, 0. <https://doi.org/>



**Copyright:** © 2023 by the authors. Licensee MDPI, Basel, Switzerland. This article is an open access article distributed under the terms and conditions of the Creative Commons Attribution (CC BY) license (<https://creativecommons.org/licenses/by/4.0/>).

far as  $\sim 200 h^{-1}$  Mpc [61]. In this paper we focus on the impact of this anomaly on the  $S_8$  tension and, more importantly, on the estimation of  $\Omega_\Lambda$  from SNe Ia data.

The relativistic viewpoint [39] is that such deviations from the Hubble flow should be thought of as variations in the expansion velocity field of the universe, rather than as ‘peculiar velocities’ w.r.t. an uniformly expanding space of the ‘background cosmology’, which is assumed *a priori* to be described by the Friedmann-Lemaître equations. However it is the latter approach that has become standard in cosmology, in particular for measuring the Hubble expansion rate. Type Ia supernova data for example are analysed in the framework of concordance cosmology (e.g. [6]) by making special relativistic corrections based on models of the local peculiar velocity field. For example in order to obtain the ‘cosmological’ redshift from the measured value, corrections are made for (non-Hubble) velocities using eq. (1). These are typically a few hundreds of  $\text{km s}^{-1}$ , so would appear to only be relevant at low redshift  $z \lesssim 0.1$ . However they can affect the analysis at higher redshift too, since evidence for accelerated expansion is a dimming of the high redshift SNe in relation to the low redshift SNe [46,49]. Moreover the local velocity field is quite noisy, reflecting our rather inhomogeneous neighbourhood, and it is not clear exactly where the separation should be made between the nearby and distant universe. Various empirical methods for accounting for peculiar velocities have thus been proposed [29]; the above problem has often been circumvented by simply excluding from cosmological fits all the SNe Ia at low redshifts. However this severely deprecates the sample statistics (since about a quarter of all known SNe Ia are in fact very local) and moreover it is somewhat arbitrary, e.g. cuts have been applied at both  $z = 0.01$  and at  $z = 0.025$  [14]. Another option is to allow for an *uncorrelated*, and somewhat arbitrary, dispersion in the velocities of SNe Ia, e.g. Perlmutter et al. [46] took the redshift uncertainty due to peculiar velocities to be  $c\sigma_z = 300 \text{ km s}^{-1}$ , while Riess et al. [49] used  $c\sigma_z = 200 \text{ km s}^{-1}$ .

The alternative is to *correct* for the peculiar velocities [42]: for this purpose the IRAS PSCZ catalogue [52], the SMAC catalogue of clusters [29] and the 2M++ catalogue [8] have all been used to infer the peculiar velocity field from the underlying density field. However these catalogues are rather limited and can be biased, moreover linear Newtonian perturbation theory is used, hence the extracted velocities are model dependent. Furthermore, these analyses *assume* convergence to the CRF at  $\gtrsim 100h^{-1}$  Mpc, as is expected in the framework of the standard  $\Lambda$ CDM model, even though this is contradicted by many independent observations [10,20,28,29,35,37,60,61]. It is in any case inappropriate to use standard  $\Lambda$ CDM to make such corrections since the model is itself a subject of the test being carried out.

Specifically in analyses of the SDSS-II/SNLS3 Joint Lightcurve Analysis (JLA) catalogue of 740 SNe Ia [3], and the subsequent Pantheon catalogue of 1048 SNe Ia (which includes 279 SNe Ia from Pan-STARRS1) [53], the low redshift SNe Ia have been retained in the cosmological fits by thus “correcting” the individual redshifts and magnitudes of the SNe for the local ‘bulk flow’ inferred from density field surveys out to  $z \sim 0.04$  [29] and  $z \sim 0.067$  [8]. However as noted by [12], in both analyses SNe Ia immediately outside the survey volume of the peculiar velocity field were arbitrarily assumed to be at rest with respect to the cosmic rest frame, despite the fact that the same surveys detected a bulk flow extending *beyond* the survey volume of  $372 \pm 127 \text{ km s}^{-1}$  and  $159 \pm 23 \text{ km s}^{-1}$ , respectively. Moreover the JLA and Pantheon analyses adopted different values of  $150 \text{ km s}^{-1}$  and  $250 \text{ km s}^{-1}$  respectively for the dispersion  $c\sigma_z$  of the bulk flow velocity.

Moreover the peculiar velocity corrections applied to both JLA and Pantheon contain significant errors and inconsistencies [12,48]. Since the covariance matrices for peculiar velocity corrections have not been provided separately, the impact of these errors on cosmological parameter estimation is hard to quantify. It should also be of concern that the the residual bulk flows of the peculiar velocity surveys align approximately with the directions of maximum hemispherical asymmetry in the sky coverage of the two catalogues.

On the theoretical side, the *correlated* fluctuations of SNe Ia magnitudes due to peculiar velocities and the impact on cosmological parameter estimation of making such corrections

have been extensively studied [16,30,32,42]. However all these studies assumed that the peculiar velocity statistics are those expected around a *typical* (aka Copernican) observer in a  $\Lambda$ CDM universe. Such an observer should in fact not observe a bulk flow exceeding  $\sim 200 \text{ km s}^{-1}$  beyond  $100 h^{-1} \text{ Mpc}$  ( $z \simeq 0.033$ ), independently of the form of the matter power spectrum [31], so clearly this assumption is in tension with reality. In this work, we use a cosmological N-body simulations to examine the validity of the peculiar velocity covariances proposed by Hui & Greene [30] in the light of additional information about our peculiar local Universe.

The bulk flow observations suggest that we are *not* typical observers in a  $\Lambda$ CDM universe [24,25,47]. We discuss here the correlated fluctuations of SNe Ia magnitudes and redshifts due to the peculiar velocities and bulk flows in and around ‘Local Universe (LU)-like’ environments in the  $z = 0$  halo catalogue of the DarkSky  $\Lambda$ CDM simulations [57]. We find that previous theoretical predictions [30] for randomly selected typical observers have *underestimated* the actual covariances for observers like ourselves by a factor of 2–8.

Next we discuss (§ 2) the peculiar velocity corrections employed in JLA [3] and show that these are both arbitrary and incomplete (§ 2.1). We compare the magnitude of the velocities used for the corrections in JLA against those obtained from the CosmicFlows-3 (CF3) compilation [59] and demonstrate that the JLA values are *underestimated* by  $\sim 48\%$  on average. We also review the various relevant sources of uncertainties and dispersions that go into the JLA cosmological fits. We then explore (§ 2.2) various methods to fit for the extent of the bulk flow in the LU and present our likelihood analysis (§ 2.3). This is followed by a discussion of related work (§ 4). An Appendix presents the standard methodology of cosmology with supernovae (§ A), and the JLA catalogue (§ B).

We find that for any consistent treatment of the peculiar velocities (including ignoring them altogether), the JLA dataset favours  $\Omega_\Lambda \lesssim 0.4$  and is consistent with a non-accelerating Universe at  $\sim 2\sigma$ . Larger values of  $\Omega_\Lambda$  which have been found in other analyses of the JLA catalogue [43,50] are in fact due to the incomplete peculiar velocity “corrections” applied. We demonstrate that, consistent with the recent finding from the CosmicFlows-4 survey [61], the JLA data favour a fast ( $> 250 \text{ km s}^{-1}$ ) bulk flow extending out to  $> 200 h^{-1} \text{ Mpc}$ , which is quite unexpected in the standard  $\Lambda$ CDM model.

Subsequently (§ 3), we examine the  $S_8$  parameter inferred by the randomly selected Copernican observers as well as the constrained ‘Local-Universe like’ observers by comparing the peculiar velocities around them with those expected from the density field. While the spread in the value of  $S_8$  inferred by Copernican observers is already larger than the disagreement between the measurement by Boruah et al. [5] and the  $\Lambda$ CDM fiducial value from Planck, LU-like observers see an additional downward bias on  $S_8$  and a larger cosmic variance.

## 2. Selecting local Universe like environments

Making the usual assumption that the CMB dipole is due to our motion wrt the CRF (aka ‘CMB frame’) in which the universe looks isotropic, so the luminosity distance  $d_L$  is related to the redshift  $z$  as in eq.(A2), the redshift of a supernova in the heliocentric frame  $z_{\text{hel}}$  (obtained by correcting the actually measured redshift for the Earth’s motion around the Sun) is related to its redshift  $z$  in the CMB frame (sometimes labelled  $z_{\text{CMB}}$ ) as [16]:

$$1 + z_{\text{hel}} = (1 + z_\odot) \times (1 + z_{\text{SN}}) \times (1 + z) , \quad (1)$$

where  $z_\odot$  is the redshift induced by our motion w.r.t. the CMB and  $z_{\text{SN}}$  is the redshift due to the peculiar motion of supernova host galaxy in the CMB frame. The luminosity distance is similarly corrected as:

$$d_L(z_{\text{hel}}) = d_L(z)(1 + z_\odot) \times (1 + z_{\text{SN}})^2 \quad (2)$$

to obtain  $d_L$  as a function of  $z$  (eq.A2) for the standard  $\Lambda$ CDM model (see Appendix A). The covariance of SNe Ia magnitudes due to peculiar velocities is then given by [16,30,32]:

$$S_{ij} = \langle \delta m_i \delta m_j \rangle = \left[ \frac{5}{\ln 10} \right]^2 \frac{(1+z_i)^2}{H(z_i)d_L(z_i)} \frac{(1+z_j)^2}{H(z_j)d_L(z_j)} \xi_{ij}, \quad (3)$$

where

$$\xi_{ij} = \langle (\vec{v}_i \cdot \hat{n}_i)(\vec{v}_j \cdot \hat{n}_j) \rangle = \frac{dD_i}{d\tau} \frac{dD_j}{d\tau} \int \frac{dk}{2\pi^2} P(k, a=1) \times \sum_l (2l+1) j_l'(k\chi_i) j_l'(k\chi_j) P_l(\hat{n}_i \cdot \hat{n}_j). \quad (4)$$

Here  $D_i$  is the linear structure growth factor at the redshift of the  $i^{\text{th}}$  SNe,  $j_l'$  is the derivative of the  $l^{\text{th}}$  spherical Bessel function and  $P_l$  is the Legendre polynomial of order  $l$ . Note that according to this expression the covariance in magnitudes between two SNe depends only on their relative angular separation (which comes in through  $P_l$ ) and is independent of their absolute directions.

N-body simulations can be used to estimate  $\xi_{ij}$  (eq.3) for different assumed observers. Figure 1 compares  $S_{ij}$  evaluated using the  $\Lambda$ CDM expectation for  $\xi_{ij}$  with that read off the  $z=0$  snapshot halo catalogue of Dark Sky, a Hubble volume, trillion-particle simulation [57], for two very different classes of observers. For the ‘Copernican observer’ in Figure 1 (left), the halo containing the observer and its orientation are selected at random — such an observer sees the universe as isotropic and homogeneous. However for the constrained ‘LU-like’ observer’ (right), only halos satisfying the following criteria are considered (the first three being the same as in [25]):

- (i) The observer halo has a Milky Way (MW)-like mass, in the range  $2.2 \times 10^{11} < M_{200} < 1.4 \times 10^{12} M_\odot$  [9] for the halo mass contained within 200 kpc.
- (ii) The bulk velocity in a sphere of radius  $R = 3.125h^{-1}$  Mpc centred on the observer is  $V = 622 \pm 150 \text{ km s}^{-1}$
- (iii) A Virgo-cluster like halo of mass  $M = (1.2 \pm 0.6) \times 10^{15} h^{-1} M_\odot$  is present at a distance  $D = 12 \pm 4h^{-1}$  Mpc from the observer.
- (iv) The angle between the bulk flow of (ii) and the direction to the Virgo-like halo of (iii) is  $(44.5 \pm 5)^\circ$ .
- (v) The bulk velocity in a sphere of  $R = 180h^{-1}$  Mpc centered on the observer is  $260 \pm 100 \text{ km s}^{-1}$  [10].
- (vi) The angle between the bulk flow of (v) and the direction to the Virgo-like halo of (iii) is  $(69.9 \pm 7.5)^\circ$ .
- (vii) The angle between the bulk flows of (ii) and (v) is  $(35.6 \pm 7.5)^\circ$ .

After an observer satisfying the above criteria is found, the entire system is rotated so that the direction of the bulk flow of criterion (ii) and the direction to the Virgo-like halo of criterion (iii) correspond to the real observed directions. The criterion on the bulk flow direction is exact, while the criterion on the direction to the Virgolike halo is imposed only on the azimuthal angle in a coordinate system in which the  $z$ -axis points towards the bulk flow direction. Criterion (iv) then suffices to orient the system. Note that the angular tolerances in (iv), (vi) and (vii) are set to be less stringent than current observational constraints, in order to limit the required computation time.

Subsequently, halos around the observer closest to the 3D coordinates of each JLA supernova are identified, and their velocities are queried. From these velocities,  $\xi_{ij}$  can be calculated. For the typical observer of Figure 1 (left), none of the steps regarding directional orientation discussed above are considered and observers are simply picked at random. As seen in Figure 1 (right), a realistic LU-like observer sees on average correlations between the supernovae of a JLA-like catalogue that are 2–8 times *stronger* than does a typical observer.

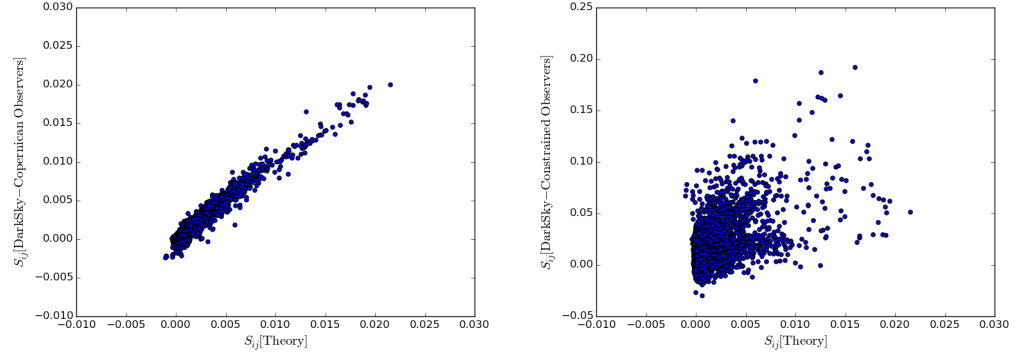


**Figure 1.** The theoretically expected covariance  $S_{ij}$  (eq.3) plotted against the value found in N-body simulations — in regions around typical observers (left) and constrained ‘Local Universe-like’ observers (right). Each point is an average over 1000 observers.

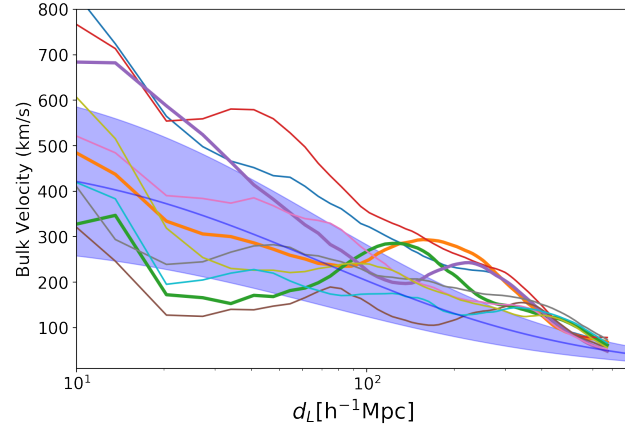


**Figure 2.** The bulk flow velocity profiles around 10 random ‘local Universe-like’ observers satisfying the criteria in § 2. Note that the velocity profile around an individual observer need not decrease monotonically, even though the ensemble average in the  $\Lambda$ CDM model (dark blue curve) does so. The shaded blue region is the  $\pm 1\sigma$  band around the mean value.

Thus the theoretical covariances of Hui & Greene [30], as given in eq.(4), is valid only for idealised observers who see neither a local bulk flow nor a preferred orientation in the sky.

### 2.1. Peculiar velocity corrections in JLA

It had been noted in Ref. [12] that the peculiar velocity ‘corrections’ applied to the SNe Ia redshifts and magnitudes in the JLA catalogue (see § B) are neither consistent nor complete. SNe Ia immediately beyond  $z \sim 0.06$  were taken to be stationary w.r.t. the CMB and assumed to only have an uncorrelated velocity dispersion  $c\sigma_z = 150 \text{ km s}^{-1}$  in the cosmological fits, even though observations of clusters indicate a bulk velocity of  $372 \pm 127 \text{ km s}^{-1}$  due to sources beyond  $200h^{-1} \text{ Mpc}$  [29]. Unlike the intrinsic dispersion  $\sigma_{M_0}$  which is assumed to be redshift *independent*, the dispersion in the magnitudes as a result of the velocity dispersion is  $5\sigma_z / (z \log 10)$  i.e. the magnitudes of lower redshift supernovae are selectively more dispersed. As seen in Figure 2, the typical bulk flow in a  $\Lambda$ CDM universe [see, e.g. 27] continues to much larger distances, with the velocity decreasing gradually. In some environments, the bulk velocity may even *increase* beyond a certain scale (as seen in the recent CosmicFlow-4 survey [61]), although the overall trend is a decreasing one.

The CosmicFlows-3 (CF3) [59] compilation presents actual measurements of the peculiar velocities of 17,669 nearby galaxies, using various *independent* distance estimators such as the Tully-Fisher relationship. In Figure 3, we compare the velocities that have been used to correct the JLA redshifts with the velocities obtained from the CosmicFlows-3



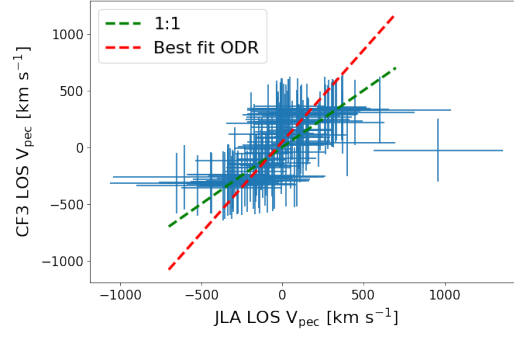


**Figure 3.** The line-of-sight velocity of SNe Ia inferred from their  $z_{\text{hel}}$  and  $z_{\text{CMB}}$  values quoted by JLA, plotted versus the line-of-sight component of the velocity of the group the object belongs to in the CF3 dataset ( $\langle V_{\text{cmb}} \rangle - gp$ ). The horizontal bars are the diagonal errors in the JLA cosmology fit (statistical plus systematic), while the vertical bars indicate the random error of  $250 \text{ km s}^{-1}$  in the CF3 measurement. The green dashed line indicates when the two are equal, while the red dashed line shows the best-fit orthogonal distance regression which has a slope of 1.61, i.e. the JLA velocities have been underestimated on average by 48%. (Note that the outlier (SN1992bh) has a peculiar velocity of  $\sim 1000 \text{ km s}^{-1}$  according to JLA, but zero according to the CF3.)

compilation. The galaxy in the CF3 dataset corresponding to a JLA supernova is identified by cross-matching with a tolerance of  $0.01^0$ , using the tool `k3match`; Out of 119 JLA SNe Ia at  $z_{\text{cmb}} < 0.06$ , 112 have CF3 counterparts within  $0.01^0$ . It is seen from the regression line [4] in Figure 3 that peculiar velocities have been systematically *underestimated* by 48% in the corrections applied in the JLA analysis [3], compared to the actual measurements by CF3.

### 2.2. Fitting for a bulk flow

We consider two illustrative profiles for the bulk flow velocity: an exponentially falling one,

$$\langle v \rangle = Pe^{-d_L/Q}, \quad (5)$$

where  $Q$  is the scale of the flow, and a linearly falling one,

$$\langle v \rangle = P - Q'd_L, \quad (6)$$

where  $Q'$  is a (dimensionless) scale parameter. In the latter parametrisation we ensure that the velocity never goes negative by setting it to zero above  $d_L = P/Q'$  (see Figure 4). The free parameters  $P$  and  $Q$  or  $Q'$  in our modelling of the bulk flow can be determined along with the 10 other usual free parameters used to fit SNe Ia data.

The effect of a bulk flow term is to modify the distance modulus of eq.(A1) such that:

$$\Delta m^{\text{bulk}}(P, Q, z_i) = -\left(\frac{5}{\ln 10}\right) \frac{(1+z_i)^2}{H(z_i)d_L(z_i)} \hat{n}_i [Pe^{-d_L(z_i)/Q}], \quad (7)$$

for the exponentially falling bulk flow, and likewise for the linearly falling bulk flow with the expression from eq.(6) now substituted in the square brackets.

### 2.3. The likelihood analysis

We can now rewrite  $z_{\text{SN}}$  and  $z$  in eq.(1) as functions of  $z_{\text{hel}}$ ,  $P$  and  $Q$  for the exponential (eq.5) or  $Q'$  for the linear (eq.6) bulk flow models respectively. A Maximum Likelihood Estimator [43] is then used with the two additional parameters  $P$  and  $Q$  (or  $Q'$ ) for the bulk flow, in addition to the usual light curve fitting parameters in the SALT2 template [3]:  $\alpha, x_{1,0}, \sigma_{x_{1,0}}, \beta, c_0, \sigma_{c_0}, M_0, \sigma_{M_0}$ . Along with the two  $\Lambda$ CDM model parameters  $\Omega_m$  and  $\Omega_\Lambda$  we then have 12 parameters in total. As shown in Table 1, the following fits are performed (including an additional dispersion of  $c\sigma_z = 150 \text{ km s}^{-1}$  as recommended by [3]):

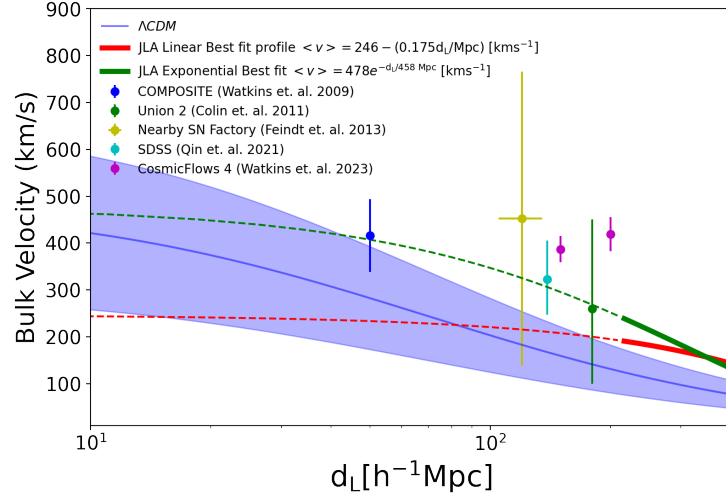


**Figure 4.** The profile of bulk flow expected in a  $\Lambda$ CDM Universe using a top-hat window function is shown as the solid blue line, while the shaded region shows the  $\pm 1\sigma$  range. Several discrepant measurements (with  $\pm 1\sigma$  uncertainties) using various surveys are shown for comparison. The red and green lines show, respectively, the linear and exponential fits to the bulk flow using JLA data (respectively rows (ix) and (x) of Table 1), along with the (blue) SN-by-SN corrections using CF3 data at smaller distances (the dashed lines indicate the extrapolated fits).

1. The same 10-parameter fit as in [43], using only the  $z_{\text{CMB}}$  values provided by JLA.
2. The 10-parameter fit using  $d_L(z_{\text{CMB}}, z_{\text{hel}}) = [(1 + z_{\text{hel}})/(1 + z_{\text{CMB}})]d_L(z_{\text{CMB}})$  — as used by [16] — and the JLA provided  $z_{\text{hel}}$  and  $z_{\text{CMB}}$  values.
3. 10-parameter fit as in (i), using only  $z_{\text{hel}}$  values (JLA provided) as was done in supernova analyses until 2011.
4. 10-parameter fit as in (i), using JLA provided  $z_{\text{hel}}$  values, after subtracting out bias corrections to  $m_B^*$ .
5. Exponentially falling bulk flow: 12-parameter fit (including the  $P$  and  $Q$  parameters of eq.(5), using only JLA provided  $z_{\text{hel}}$  values. No peculiar velocity corrections are applied.
6. Linearly falling bulk flow: 12-parameter fit (including the  $P$  and  $Q$  parameters of eq.(6) using only JLA provided  $z_{\text{hel}}$  values. No peculiar velocity corrections are applied.
7. JLA corrected redshifts + Exponential bulk flow: 12-parameter fit: SNe with peculiar velocity corrections applied by JLA, are treated as in (ii) above, while an exponentially falling bulk flow is fitted to the remaining SNe.
8. JLA corrected redshifts + Linear bulk flow: As in (vii), but with the linear parametrisation of the bulk flow.
9. CF-3 data & the Exponential bulk flow fit: 12-parameter fit using eq.(2) with the CF3-derived values of  $z_{\text{hel}}$  and  $z_{\text{CMB}}$  (see § 2.1) used for the low  $z$  SNe Ia to which the velocity correction can be applied. For the remaining objects, we use the JLA  $z_{\text{hel}}$  values, and an Exponential bulk flow is fitted using eq.(5) as described above.
10. CF-3 data & the Linear bulk flow fit: 12-parameter fit using eq.(6) with the CF3-derived values of  $z_{\text{hel}}$  and  $z_{\text{CMB}}$  (see § 2.1) used for the low  $z$  SNe Ia to which the velocity correction can be applied. For the remaining objects, we use the JLA  $z_{\text{hel}}$  values, and a Linear bulk flow is fitted using eq.(6).

In all these fits, the direction of the bulk flow is fixed to be in the CMB dipole direction as most previous analyses have shown large dipoles at intermediate redshifts converging to this direction [10,11,35,47,60]. In Table 1 we also show the fit results after imposing the additional constraint of ‘No acceleration’ for a  $\Lambda$ CDM Universe i.e.:  $q_0 \equiv \Omega_\Lambda/2 - \Omega_m = 0$ . For the last 2 fits we also show the effect of imposing the constraint of zero curvature (‘Flat’): i.e.  $\Omega_\Lambda + \Omega_m = 1$ .

The bulk flow fit is  $\langle v \rangle = 478e^{-d_L/458 \text{ Mpc}} \text{ km s}^{-1}$  for the exponential decay form (5), and  $\langle v \rangle = [246 - 0.175(d_L/\text{Mpc})] \text{ km s}^{-1}$  for the linearly falling form (6). Including the bulk flow *always* improves the quality of the fit as can be seen from the smaller values of  $-2 \log \mathcal{L}_{\text{max}}$ . This justifies adding the 2 parameters characterising it. In all the above fits apart from the ‘No acceleration’ ones, the best-fit bulk flow extends beyond  $200h^{-1} \text{ Mpc}$  at  $250 \text{ km s}^{-1}$ . Figure 4 shows our results along with selected recent observations.

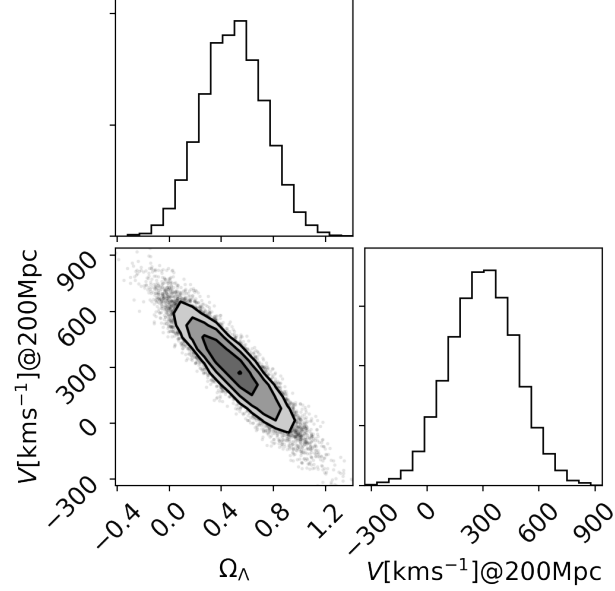


**Figure 5.** 1, 2 and 3  $\sigma$  contours corresponding to the fit (ix) of Table 1 wherein peculiar velocities from CosmicFlows-3 are used for SN-by-SN corrections and the flow is allowed to continue beyond the extent of the survey with an exponential fall-off (eq.5). The velocity of the bulk flow at a top-hat smoothing scale of radius 200 Mpc is shown in the right histogram of the posterior, while the top histogram shows the extracted value of  $\Omega_\Lambda$ .

Using the CF-3 data and the linear bulk flow fit, as well as other fits of similar quality, the difference in the goodness of fit of the best model (with the lowest value of  $-2 \log \mathcal{L}_{\text{max}}$ ) w.r.t. the corresponding ‘No acceleration’ fit is now significantly smaller compared to previous studies. Figure 5 demonstrates the degeneracy between the derived value of  $\Omega_\Lambda$  and the local bulk flow, illustrating that the latter is an *essential* nuisance parameter to be added to cosmological fits when analysing SNe Ia. Allowing for the bulk flow in the fit demonstrates that the evidence for acceleration using SNe Ia data alone is even smaller than was found previously [43].

The results in Table 1 may be summarised as follows:

- Of all the fits, the only ones favouring  $\Omega_\Lambda > 0.5$  are just those which include the incorrect and incomplete peculiar velocity ‘corrections’ of JLA [3].
- Fit (iv), which has *no* peculiar velocity corrections at all, as in the cosmic acceleration discovery papers [46] and [49], prefers  $\Omega_\Lambda = 0.396$  with  $< 2\sigma$  evidence for acceleration.
- While previous work has suggested that bulk flows should not bias  $\Omega_\Lambda$ , it in fact drops by  $\sim 30\%$  if we undo the peculiar velocity ‘corrections’ of JLA and instead use the kinematic data from CF3. This illustrates the huge impact of considering a realistic LU-like observer such as ourselves, rather than the randomly located observer assumed in all previous analyses [16,30,32,42]. In particular this contradicts what is stated in Table 11 of [3].

The discovery papers [46] and [49] assumed the uncertainty due to peculiar velocities to be  $c\sigma_z = 300 \text{ km s}^{-1}$  and  $200 \text{ km s}^{-1}$  respectively, but neither made SN-by-SN corrections.



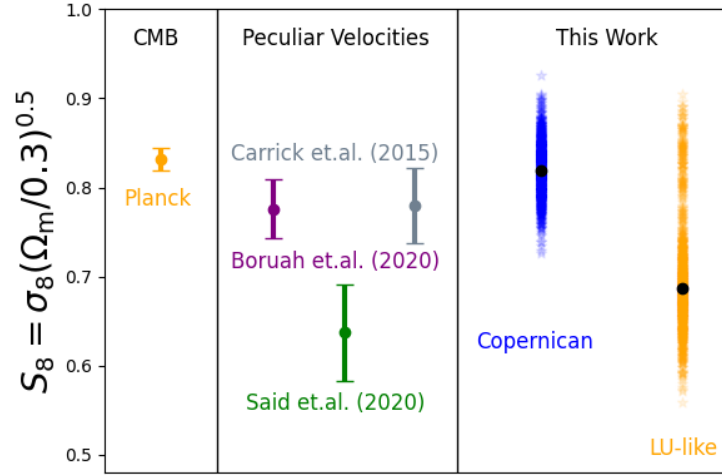


**Figure 6.** Distribution of the  $S_8$  parameter extracted by comparing the ‘observed’ (in this case, simulated) peculiar velocity with the prediction from the density contrast field, for 1000 observers selected at random (Copernican) as well as selected to be in local Universe-like (LU-like) environments. The median values are shown in black. For comparison, the actual measurement [5] made using the same method is shown, as well as the value derived from the CMB.

The JLA [3] and Pantheon [53] analyses employ *incorrect* peculiar velocity ‘corrections’, together with redshift uncertainties of  $c\sigma_z = 150 \text{ km s}^{-1}$  and  $250 \text{ km s}^{-1}$  respectively.

### 3. Extracting $S_8$

The peculiar velocity field  $\mathbf{v}(\mathbf{r})$  is defined as

$$\mathbf{v}(\mathbf{r}) = \frac{H_0 f(\Omega_m)}{4\pi} \int d^3\mathbf{r}' \delta(\mathbf{r}') \frac{(\mathbf{r}' - \mathbf{r})}{|\mathbf{r}' - \mathbf{r}|^3}, \quad (8)$$

where  $f(\Omega_m)$  is the logarithmic growth rate of fluctuations ( $\simeq \Omega_m^{0.55}$  in the  $\Lambda$ CDM model) and  $\delta(\mathbf{r})$  is the matter density contrast field:

$$\delta(\mathbf{r}) = \frac{\rho(\mathbf{r}) - \bar{\rho}}{\bar{\rho}}. \quad (9)$$

The density in the above equation is that of gravitating matter, which is dominated by unobservable dark matter in the standard paradigm. It is usually assumed that observed luminous objects trace out the underlying matter density contrast with only linear bias

$$\delta_g = b_g \delta \quad (10)$$

where  $b_g$  and  $\delta_g$  are the bias and the density fluctuation field of the tracers respectively. The predicted peculiar velocity field

$$\mathbf{v}_{\text{pred}}(\mathbf{r}) = \frac{H_0}{4\pi} \int d^3\mathbf{r}' \delta_t(\mathbf{r}') \frac{(\mathbf{r}' - \mathbf{r})}{|\mathbf{r}' - \mathbf{r}|^3} \quad (11)$$

can now be compared to the ‘observed’ (in the case of the present study, simulated) to estimate the term  $\beta_t$

$$\beta_t = \frac{\mathbf{v}_t}{\mathbf{v}_{\text{pred}}} \quad (12)$$

for the tracer  $t$  [5,26]. Thus  $\beta_t$  can be obtained by fitting a large number of measured tracer velocities against the predictions from the density field. We convert this, as in

[5], to  $S_8 \equiv \sigma_8(\Omega_m/0.3)^{0.5}$ , using the input value of  $\Omega_m = 0.2952$  used for the Dark Sky simulations.

In practice, the observational tracers used to map the velocity field need not be the same as are used to map the density field; in fact they usually are not [5]. However, since our aim is to study the effect of the local environment on velocity-density correlations, we use the same tracers for both, viz. the halos. (We use halos rather than particles since the  $z = 0$  halo catalogue of Dark Sky is computationally more tractable than the  $z = 0$  particle snapshot.) In order to keep our study as similar as possible to Ref.[26] we use a Gaussian kernel with a smoothing length of  $5 h^{-1}$  Mpc to smooth out the density fluctuation field.

It is evident from Figure 6 that there is a downward bias in measurements of  $S_8$  by local Universe-like observers such as ourselves and the cosmic variance is also higher. This may well account for the tension between the value derived from Planck data, and that obtained by comparing the reconstructed velocity field from the 2M++ galaxy redshift compilation to supernovae, Fundamental Plane and Tully–Fisher distance catalogues [5,8,51].

#### 4. Discussion

Other authors [32,33] have come to different conclusions regarding the impact of the bulk flow on cosmological parameter determination so we comment on why this is so. In general relativity space-time evolves according to the Einstein field equations but for simplicity and tractability, structure formation is studied by linearising these around the maximally symmetric FLRW solution. Further making restricted ‘gauge’ choices [2], cosmological reality is simulated using *Newtonian* N-body simulations wherein there is a background space that expands homogeneously and isotropically, governed by just one scale factor, while density perturbations evolve around this background according to Newtonian gravity. However solutions to the linearised field equations can only be linearisations of the solutions to the fully non-linear equations [17,41] hence this approach hides known physical phenomena. Indeed a relativistic universe exhibits locally inhomogeneous expansion *beyond* that evident in linear perturbation theory around a maximally symmetric background [22]. It was therefore proposed to consider the expansion of the Universe at late times as an *average* effect, arising out of the coarse-graining of physics at smaller scales [7]. Peculiar velocities thus form the key frontier between the real Universe and that which is modelled usually by 1st-order perturbation of the fluid equations or in a Newtonian N-body simulation. Note that in the real Universe peculiar velocities are differences in the expansion rate of the Universe at different space-time points, while in a N-body simulation they arise *by construction* from Newtonian gravity acting on top of a hypothetical uniformly expanding space. Now Ref.[32] uses (just as [30]), the restricted longitudinal or conformal-Newtonian ‘gauge’ [2] to derive the covariance (eq.3) for a typical observer. But as Figure 1 shows this would be relevant for observational cosmology only if each SNe Ia were being observed from a *different*, randomly sampled host galaxy. In practice we observe the real Universe from only one vantage point. Nevertheless Ref.[32] adds this covariance as a “guaranteed theoretical signal” to the uncertainty budget of the JLA data, thus weakening the statistical preference for a bulk flow to  $\lesssim 2\sigma$  (as seen in their Figure 4).

Ref.[33] claims further that any bias in the inference of dark energy parameters due to the effect of peculiar velocities can be determined *a priori* via simulations. This misses the point however that  $\Lambda$ CDM is a model and N-body simulations contain only as much physics as has been coded into them, i.e. neither captures the real Universe.

#### 5. Conclusions

To summarise, we are *not* typical (Copernican) observers — we are embedded in a fast and deep bulk flow and this has significant impact on the covariances used in supernova cosmology.<sup>1</sup> We have studied the effect on SNe Ia redshifts in the JLA catalogue

<sup>1</sup> There are other corrections too such as for gravitational lensing, which become more important than the effect of peculiar velocities at a redshift  $z > 0.15$  — see Figure B.1 of [12].

**Table 1.** Best-fit parameters and results for the fits described in § 2.3 using the Maximum Likelihood Estimator [44]. Including the bulk flow improves the quality of the fit and decreases the significance of accelerated expansion, as seen from the decrease of  $-2 \log \mathcal{L}_{\max}$ . Note that "No acceleration" corresponds to  $\Omega_\Lambda = \Omega_m/2$ .

	Fit	$-2 \log \mathcal{L}_{\max}$	$\Omega_m$	$\Omega_\Lambda$	$\alpha$	$x_{1,0}$	$\sigma_{x_{1,0}}$	$\beta$	$c_0$	$\sigma_{c_0}$	$M_0$	$\sigma_{M_0}$	$V$ (km s $^{-1}$ ) @200h $^{-1}$ Mpc
(i)	[43]	-214.97	0.341	0.569	0.134	0.0385	0.931	3.059	-0.016	0.071	-19.052	0.108	-
	No acceleration	-203.93	0.068	0.034	0.132	0.0327	0.932	3.045	-0.013	0.071	-19.006	0.110	-
(ii)	[43] + JLA $z$	-221.93	0.340	0.565	0.133	0.0385	0.932	3.056	-0.016	0.071	-19.051	0.107	-
	No acceleration	-210.99	0.070	0.035	0.131	0.0328	0.932	3.042	-0.013	0.071	-19.006	0.109	-
(iii)	No pec. vel. corr. to $z$	-215.40	0.285	0.483	0.134	0.0398	0.932	3.038	-0.016	0.071	-19.051	0.108	-
	No acceleration	-207.67	0.051	0.025	0.132	0.0348	0.932	3.023	-0.014	0.071	-19.012	0.110	-
(iv)	No pec. vel. corr. to $z$ or $m_B$	-216.89	0.235	0.396	0.135	0.0397	0.932	3.029	-0.016	0.071	-19.040	0.109	-
	No acceleration	-211.84	0.0413	0.021	0.133	0.0357	0.932	3.016	-0.014	0.071	-19.008	0.110	-
(v)	Exponential bulk flow	-217.51	0.289	0.452	0.134	0.0390	0.932	3.036	-0.016	0.071	-19.037	0.107	253
	No acceleration	-211.3	0.077	0.039	0.132	0.0347	0.932	3.024	-0.014	0.071	-19.002	0.108	292
(vi)	Linear bulk flow	-217.47	0.290	0.455	0.134	0.0390	0.932	3.036	-0.016	0.071	-19.038	0.107	265
	No acceleration	-211.99	0.082	0.041	0.132	0.0347	0.932	3.025	-0.014	0.071	-19.002	0.108	282
(vii)	JLA + Exp. bulk flow	-224.87	0.340	0.570	0.133	0.0387	0.932	3.051	-0.016	0.072	-19.052	0.107	271
	No acceleration	-216.3	0.077	0.039	0.132	0.0347	0.932	3.024	-0.014	0.071	-19.002	0.108	295
(viii)	JLA + Lin. bulk flow	-225.08	0.341	0.577	0.133	0.0387	0.932	3.050	-0.016	0.071	-19.054	0.107	238
	No acceleration	-214.14	0.072	0.036	0.131	0.0328	0.932	3.041	-0.013	0.071	-19.005	0.109	251
(ix)	CF3 + Exp. Bulk Flow	-225.61	0.279	0.427	0.133	0.0386	0.932	3.001	-0.016	0.071	-19.034	0.109	309
	No acceleration	-220.72	0.086	0.043	0.132	0.0346	0.932	2.990	-0.015	0.071	-19.001	0.110	398
	Flat	-223.96	0.393	0.607	0.133	0.0357	0.933	2.998	-0.016	0.071	-19.045	0.110	338
(x)	CF3 + Lin. bulk flow	-225.73	0.277	0.431	0.133	0.0386	0.932	3.002	-0.016	0.071	-19.037	0.109	211
	No acceleration	-220.16	0.085	0.042	0.132	0.0346	0.932	2.991	-0.015	0.071	-19.001	0.110	249
	Flat	-224.18	0.390	0.610	0.134	0.0399	0.932	3.006	-0.016	0.071	-19.047	0.109	215

of the peculiar velocities of their host galaxies. Using direct measurements of these from CosmicFlows-3, we find that the effect of peculiar velocities for low redshift SNe Ia has been underestimated by 48%. We show that the usual procedure of adding a constant velocity dispersion of a few hundred km s $^{-1}$  to account for peculiar velocities at high redshift, does not take into account the *correlated* flow of the galaxies. By analysing the DarkSky simulation [57] we demonstrate that ‘Local Universe-like’ observers like ourselves see 2–8 times stronger correlation between the SNe Ia than a randomly located observer does. The JLA analysis [3] corrected the data assuming the CMB dipole to be entirely kinematic in origin and that convergence to the CMB rest frame occurs abruptly at redshift  $z \sim 0.06$ . Since neither assumption is fully supported by observations, we have adopted a general model of the bulk flow which introduces two extra parameters in the analysis. We do not either adopt the  $\Lambda$ CDM model *a priori*, nor do we make assumptions about the origin of the CMB dipole. This provides an independent estimate of the bulk flow and we find that it persists out to distances beyond 200  $h^{-1}$ Mpc, with a speed of  $\sim 250$  km s $^{-1}$ . Our maximum likelihood analysis then shows that the accelerated expansion of the Universe cannot be inferred as a statistically significant result from the SNe Ia data alone.

## Appendix A Supernova Cosmology

The largest public catalogues of SNe Ia lightcurves, the JLA [3] and its successor Pantheon [53], employ the ‘Spectral Adaptive Lightcurve Template 2’ (SALT2) to fit each SNe Ia light curve with 3 parameters: the apparent magnitude  $m_B^*$  (at maximum in the rest frame ‘B-band’) and the ‘shape’ and ‘colour’ corrections,  $x_1$  and  $c$  [23]. (A ‘host galaxy mass correction’ may also be included, however the Maximum Likelihood Estimator is insensitive to this parameter [44].) The distance modulus is then:

$$\mu_{\text{SN}} = m_B^* - M + \alpha x_1 - \beta c, \quad (\text{A1})$$

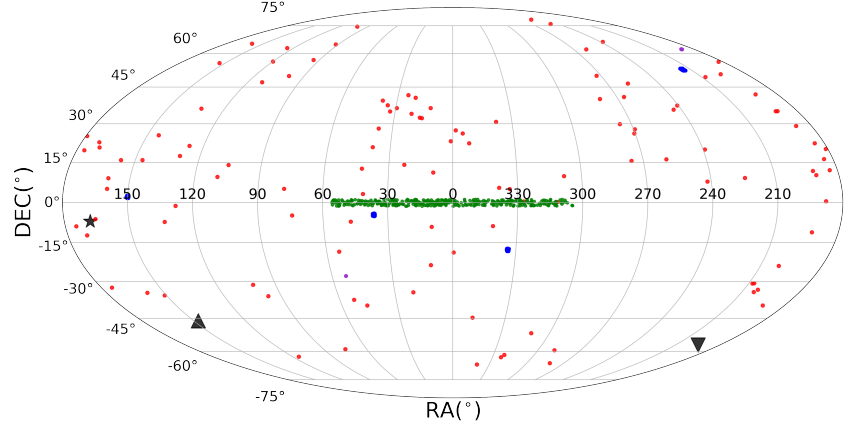


**Figure A1.** Sky distribution (Mollweide projection, equatorial coordinates) of the 4 subsamples of the JLA catalogue: low  $z$  (red dots), SDSS (green dots), HST (black dots), clusters of many SNe Ia from SNLS (blue dots). The directions of the CMB dipole (star), the SMAC bulk flow (triangle) [42], and the 2M++ bulk flow (inverted triangle) [8] are shown in grey.

where  $\alpha$  and  $\beta$  are assumed to be constants, as is  $M$  the absolute SNe Ia magnitude, as befits a ‘standard candle’. In the standard  $\Lambda$ CDM cosmological model this is related to the luminosity distance  $d_L$  as:

$$\begin{aligned}
 \mu &\equiv 25 + 5 \log_{10}(d_L/\text{Mpc}), \quad \text{where:} \\
 d_L &= (1+z) \frac{d_H}{\sqrt{\Omega_k}} \sin\left(\sqrt{\Omega_k} \int_0^z \frac{H_0 dz'}{H(z')}\right), \text{ for } \Omega_k > 0 \\
 &= (1+z) d_H \int_0^z \frac{H_0 dz'}{H(z')}, \text{ for } \Omega_k = 0 \\
 &= (1+z) \frac{d_H}{\sqrt{\Omega_k}} \sinh\left(\sqrt{\Omega_k} \int_0^z \frac{H_0 dz'}{H(z')}\right), \text{ for } \Omega_k < 0 \\
 d_H &= c/H_0 \simeq 3000h^{-1} \text{ Mpc}, H_0 \equiv 100h \text{ km s}^{-1} \text{ Mpc}^{-1}, \\
 H &= H_0 \sqrt{\Omega_m(1+z)^3 + \Omega_k(1+z)^2 + \Omega_\Lambda}.
 \end{aligned} \tag{A2}$$

Here  $H$  the Hubble parameter ( $H_0$  being its present value),  $d_H$  is the ‘Hubble distance’ and  $\Omega_m, \Omega_\Lambda, \Omega_k$  are the matter, cosmological constant and curvature densities in units of the critical density. In the standard  $\Lambda$ CDM model these are related by the ‘cosmic sum rule’:  $1 = \Omega_m + \Omega_\Lambda + \Omega_k$ , which is simply rewriting the Friedmann equation.

Thus knowing the redshift and distance of the ‘standardised’ SNe Ia, one can determine the cosmological parameters. However these are measured from Earth and usually quoted in the heliocentric frame (allowing for the Earth’s motion around the Sun), so need to first be translated to the reference frame in which the universe is (statistically) isotropic and homogeneous and the above equations hold. Assuming that the CMB dipole is purely kinematic in origin, this is taken to be the ‘CMB frame’ which can be reached by a local special relativistic boost, so the measured values are corrected as in eq.(1) for the redshift and eq.(2) for the luminosity distance.

## Appendix B The Joint Lightcurve Analysis catalogue

The JLA catalogue [3] consists of 740 spectroscopically confirmed SNe Ia, including several low redshift ( $z < 0.1$ ) samples, three seasons of SDSS-II ( $0.05 < z < 0.4$ ) and three years of SNLS ( $0.2 < z < 1$ ) data, all calibrated consistently in the ‘Spectral Adaptive Lightcurve Template 2’ (SALT2) scheme. Figs. A1 and A2 show respectively the sky coverage and redshift distribution of this publicly available catalogue.

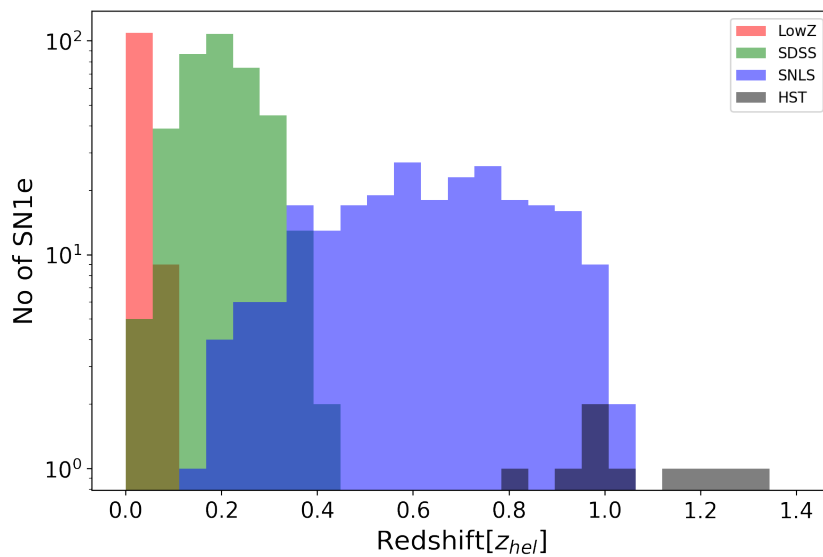


**Figure A2.** The redshift distribution of the 4 samples that make up the SDSS-II/SNLS3 Joint Lightcurve Analysis catalogue.

We use the publicly available SALT2 light curve fits done by the JLA collaboration [3] but rather than their ‘constrained’  $\chi^2$  statistic which is unprincipled, we employ the Maximum Likelihood Estimator of Nielsen et al. [43]. Our approach, is frequentist but equivalent to the ‘Bayesian Hierarchical Model’ [38,50,56]. It has been used in independent analyses of SNe Ia [15,18].

Ref.[50] advocated that the shape and colour parameters be allowed to depend on both the SNe Ia sample and the redshift, however this introduces 12 additional parameters (to the 10 used above) and thus violates the Bayesian information criterion [12,13]. [34] noted that if  $x_1$  and  $c$  evolve with redshift, the likelihood-based methods return biased values of the parameters (while the ‘constrained  $\chi^2$ ’ method continues to be robust), however this conclusion is arrived at using Monte Carlo simulations which *assume* the  $\Lambda$ CDM model and is therefore a circular argument. It has been emphasised by [15] that systematic uncertainties and selection biases in the data need to be corrected for in a model-independent manner, *before* fitting to a particular cosmological model. For further discussion of these (and related) issues see [40].

**Author Contributions:** All authors have contributed to this work and agreed to the published version of the manuscript.

**Funding:** This research received no external funding.

**Conflicts of Interest:** The authors declare no conflict of interest.

## References

1. Abdalla E.; Franco Abellán G.; Aboubrahim A.; et al. Cosmology intertwined: A review of the particle physics, astrophysics, and cosmology associated with the cosmological tensions and anomalies, *J. High Ener. Astropys.* **2022**, *34*, 49.
2. Bertschinger E. Cosmological dynamics: Course 1 **1993**, preprint [arXiv:astro-ph/9503125](https://arxiv.org/abs/astro-ph/9503125).
3. Betoule M.; Kessler R.; Guy J.; et al. Improved cosmological constraints from a joint analysis of the SDSS-II and SNLS supernova samples, *Astron. Astrophys.* **2014**, *568*, A22.
4. Boggs P. T.; Rogers J. E. Orthogonal distance regression, *Contemp. Math.* **1990**, *112*, 183.
5. Boruah S. S.; Hudson M. J.; Lavaux G. *Mon. Not. Roy. Astron. Soc.* **2020**, *498*, 2703.
6. Brout D.; Scolnic D.; Popovic B.; et al. The Pantheon+ Analysis: Cosmological Constraints, *Astrophys. J.* **2022**, *938*, 110.
7. Buchert T.; Carfora M.; Ellis G. F. R.; et al. Is there proof that backreaction of inhomogeneities is irrelevant in cosmology?, *Class. Quant. Grav.* **2015**, *32*, 215021.

8. Carrick J.; Turnbull S. J.; Lavaux G.; Hudson M. J. Cosmological parameters from the comparison of peculiar velocities with predictions from the 2M++ density field, *Mon. Not. Roy. Astron. Soc.* **2015**, *450*, 317.
9. Cautun M.; Frenk C. S.; van de Weygaert R.; Hellwing W. A.; Jones B. J. T. Milky Way mass constraints from the Galactic satellite gap, *Mon. Not. Roy. Astron. Soc.* **2014**, *445*, 2049.
10. Colin J.; Mohayaee R.; Sarkar S.; Shafieloo A. Probing the anisotropic local universe and beyond with SNe Ia data, *Mon. Not. Roy. Astron. Soc.* **2011**, *414*, 264.
11. Colin J.; Mohayaee R.; Rameez M.; Sarkar S. High redshift radio galaxies and divergence from the CMB dipole, *Mon. Not. Roy. Astron. Soc.* **2017**, *471*, 1045.
12. Colin J.; Mohayaee R.; Rameez M.; Sarkar S. Evidence for anisotropy of cosmic acceleration, *Astron. Astrophys.* **2019a**, *631*, L13.
13. Colin J.; Mohayaee R.; Rameez M.; Sarkar S. A response to Rubin & Heitlauf: "Is the expansion of the universe accelerating? All signs still point to yes", preprint **2019b**, [arXiv:1912.04257](https://arxiv.org/abs/1912.04257).
14. Conley A.; Guy J.; Sullivan M.; et al. Supernova Constraints and Systematic Uncertainties from the First 3 Years of the Supernova Legacy Survey, *Astrophys. J. Suppl.* **2011**, *192*, 1.
15. Dam L. H.; Heinesen A.; Wiltshire D. L. Apparent cosmic acceleration from type Ia supernovae, *Mon. Not. Roy. Astron. Soc.* **2017**, *472*, 835.
16. Davis T. M.; Hui L.; Frieman J. A.; et al. The effect of peculiar velocities on supernova cosmology, *Astrophys. J.* **2011**, *741*, 67.
17. D'Eath P. D. On the existence of perturbed Robertson-Walker universes, *Annals Phys.* **1976**, *98*, 237.
18. Desgrange C.; Heinesen A.; Buchert T. Dynamical spatial curvature as a fit to type Ia supernovae, *Intern. J. Mod. Phys. D* **2019**, *28*, 1950143.
19. Filippou K.; Tsagas C. G. *Astrophys. Space Sci.* **2021**, *366*, 4.
20. Feindt U.; Kerschhaggl M.; Kowalski M.; et al. Measuring cosmic bulk flows with Type Ia Supernovae from the Nearby Supernova Factory, *Astron. Astrophys.* **2013**, *560*, A90.
21. Freedman W. L. Measurements of the Hubble Constant: Tensions in Perspective, *Astrophys. J.* **2021**, *919*, 16.
22. Giblin J. T.; Mertens J. B.; Starkman G. D. Departures from the Friedmann-Lemaître-Robertson-Walker Cosmological Model in an Inhomogeneous Universe: A Numerical Examination, *Phys. Rev. Lett.* **2015**, *116*, 251301.
23. Guy J.; Astier P.; Baumont S. et al. SALT2: Using distant supernovae to improve the use of Type Ia supernovae as distance indicators, *Astron. Astrophys.* **2007**, *466*, 11.
24. Hellwing W. A.; Bilicki M.; Libeskind N. I. Uneven flows: On cosmic bulk flows, local observers, and gravity, *Phys. Rev. D* **2018**, *97*, 103519.
25. Hellwing W. A.; Nusser A.; Feix M.; Bilicki M. Not a Copernican observer: biased peculiar velocity statistics in the local Universe, *Mon. Not. Roy. Astron. Soc.* **2017**, *467*, 2787.
26. Hollinger A. M.; Hudson M. J. *Mon. Not. Roy. Astron. Soc.* **2021**, *502*, 3723.
27. Hong T.; Springob C. M.; Staveley-Smith L.; Scrimgeour M. I.; Masters K. L.; Macri L. M.; Koribalski B. S.; Jones D. H.; Jarrett T. H. 2MTF – IV. A bulk flow measurement of the local Universe, *Mon. Not. Roy. Astron. Soc.* **2014**, *445*, 402.
28. Howlett C.; Said K.; Lucey J. R.; Colless M.; Qin F.; Lai Y.; Tully R. B.; Davis T. M. The sloan digital sky survey peculiar velocity catalogue, *Mon. Not. Roy. Astron. Soc.* **2022**, *515*, 953.
29. Hudson M. J.; Smith R. J.; Lucey J. R.; Branchini E. Streaming motions of galaxy clusters within 12000 km/s. 5. The peculiar velocity field, *Mon. Not. Roy. Astron. Soc.* **2004**, *352*, 61.
30. Hui L.; Greene P. B. Correlated fluctuations in luminosity distance and the (surprising) importance of peculiar motion in supernova surveys, *Phys. Rev. D* **2006**, *73*, 123526.
31. Hunt P.; Sarkar S. Constraints on large scale inhomogeneities from WMAP-5 and SDSS: confrontation with recent observations, *Mon. Not. Roy. Astron. Soc.* **2010**, *401*, 547.
32. Huterer D.; Shafer D. L.; Schmidt F. No evidence for bulk velocity from type Ia supernovae, *J. Cosmo. Astropart. Phys.* **2015**, *12*, 033.
33. Huterer D. Specific Effect of Peculiar Velocities on Dark-Energy Constraints from Type Ia Supernovae, *Astrophys. J. Lett.* **2020**, *904*, L28.
34. Karpenka N. V. The supernova cosmology cookbook: Bayesian numerical recipes, preprint **2015**, [arXiv:1503.03844](https://arxiv.org/abs/1503.03844).
35. Cosmic flow from 2MASS redshift survey: The origin of CMB dipole and implications for LCDM cosmology, Lavaux G.; Tully R. B.; Mohayaee R.; Colombi S. *Astrophys. J.* **2010**, *709*, 48.
36. Leibundgut B. Type Ia Supernovae, *Astron. & Astrophys. Rev.* **2000**, *10*, 179.



37. Magoulas C.; Springob C.; Colless M. et al. Measuring the cosmic bulk flow with 6dFGSv, *Proc. IAU Symp.* **2016**, *308*, 336.
38. March M.; Trotta R.; Berkes P.; Starkman G.; Vaudrevange P. *Mon. Not. Roy. Astron. Soc.* **2011**, *418*, 2308.
39. McClure M. L.; Dyer C. C. Anisotropy in the Hubble constant as observed in the HST Extragalactic Distance Scale Key Project results, *New Astron.* **2007**, *12*, 533.
40. Mohayaee R.; Rameez M.; Sarkar S. Do supernovae indicate an accelerating universe?, *Eur. Phys. J. ST* **2021**, *230*, 2067.
41. Mukhanov V. F.; Feldman H. A.; Brandenberger R. H. Theory of cosmological perturbations *Phys. Rep.* **1992**, *215*, 203.
42. Neill J. D.; Hudson M. J.; Conley A. The peculiar velocities of local Type Ia supernovae and their impact on cosmology, *Astrophys. J. Lett.* **2007**, *661*, L123.
43. Nielsen J. T.; Guffanti A.; Sarkar S. Marginal evidence for cosmic acceleration from Type Ia supernovae, *Sci. Rep.* **2016**, *6*, 35596.
44. Nielsen J. T. Supernovae as cosmological probes, preprint **2015**, arXiv:1508.07850.
45. Peebles P. J. E. Anomalies in physical cosmology, *Annals Phys.* **2022**, *447*, 169159.
46. Perlmutter S.; Aldering G.; Goldhaber G. et al. Measurements of Omega and Lambda from 42 high redshift supernovae, *Astrophys. J.* **1999**, *517*, 565.
47. Rameez M.; Mohayaee R.; Sarkar S.; Colin J. The dipole anisotropy of AllWISE galaxies, *Mon. Not. Roy. Astron. Soc.* **2018**, *477*, 1772.
48. Rameez M.; Sarkar S. Is there really a Hubble tension?, *Class. Quant. Grav.* **2021**, *38*, 154005.
49. Riess A. G.; Filippenko A. V.; Challis P. et al. Observational evidence from supernovae for an accelerating universe and a cosmological constant, *Astron. J.* **1998**, *116*, 1009.
50. Rubin D.; Hayden B. Is the expansion of the universe accelerating? All signs point to yes, *Astrophys. J. Lett.* **2016**, *833*, L30.
51. Said K.; Colless M.; Magoulas C.; Lucey J. R.; Hudson M. J. Joint analysis of 6dFGS and SDSS peculiar velocities for the growth rate of cosmic structure and tests of gravity, *Mon. Not. Roy. Astron. Soc.* **2020**, *497*, 1275.
52. Saunders W.; Sutherland W. J.; Maddox S. J. et al. The PSCz catalogue, *Mon. Not. Roy. Astron. Soc.* **2000**, *317*, 55.
53. Scolnic D.M.; Jones, D.O.; Rest, A. et al. The Complete Light-curve Sample of Spectroscopically Confirmed SNe Ia from Pan-STARRS1 and Cosmological Constraints from the Combined Pantheon Sample, *Astrophys. J.* **2018**, *859*, 101.
54. Secrest N. J.; von Hausegger S.; Rameez M.; Mohayaee R.; Sarkar S.; Colin J. A Test of the Cosmological Principle with Quasars, *Astrophys. J. Lett.* **2021**, *908*, L51.
55. Secrest N. J.; von Hausegger S.; Rameez M.; Mohayaee R. and Sarkar S. A Challenge to the Standard Cosmological Model, *Astrophys. J. Lett.* **2022**, *937*, L31.
56. Shariff H.; Xiao J.; Trotta R.; van Dyk D. A. BAHAMAS: New Analysis of Type Ia Supernovae Reveals Inconsistencies with Standard Cosmology, *Astrophys. J.* **2016**, *827*, 1.
57. Skillman S. W.; Warren M. S.; Turk M. J. et al. Dark Sky Simulations: Early Data Release, preprint **2014**, arXiv:1407.2600.
58. Tsagas C. G.; Kadiltzoglou M. I.; Asvesta K. The deceleration parameter in “tilted” Friedmann universes: Newtonian vs relativistic treatment, *Astrophys. Space Sci.* **2021**, *366*, 90.
59. Tully R. B.; Courtois H. M.; Sorce J. G. Cosmicflows-3, *Astron. J.* **2016**, *152*, 50.
60. Watkins R.; Feldman H. A.; Hudson M. J. Large-scale bulk flows from the Cosmicflows-2 catalogue, *Mon. Not. Roy. Astron. Soc.* **2009**, *392*, 743.
61. Watkins R.; Allen T.; Bradford C. J.; Walker A.; Feldman H. A.; Cionitti R.; Al-Shorman Y.; Kourkchi E.; Tully R. B. Analysing the large-scale bulk flow using cosmicflows4: increasing tension with the standard cosmological model, *Mon. Not. Roy. Astron. Soc.* **2023**, *524*, 1885.

**Disclaimer/Publisher’s Note:** The statements, opinions and data contained in all publications are solely those of the individual author(s) and contributor(s) and not of MDPI and/or the editor(s). MDPI and/or the editor(s) disclaim responsibility for any injury to people or property resulting from any ideas, methods, instructions or products referred to in the content.